ORIGINAL ARTICLE

Na-alginate, polyaniline and polypyrrole composites with cellulosic biomass for the adsorptive removal of herbicide: Kinetics, equilibrium and thermodynamic studies

Amina Khan [a], Haq Nawaz Bhatti [a,*], Marrium Tahira [a], Fatimah Othman Alqahtani [b,*], Foziah F. Al-Fawzan [c], Siham A. Alissa [c], Munawar Iqbal [d]

[a] *Department of Chemistry, University of Agriculture, Faisalabad, Pakistan*
[b] *Department of Chemistry, College of Science, King Faisal University, P.O. Box 380, Al-Ahsa 31982, Saudi Arabia*
[c] *Department of Chemistry, College of Science, Princess Nourah bint Abdulrahman University, P.O. Box 84428, Riyadh 11671, Saudi Arabia*
[d] *Department of Chemistry, Division of Science and Technology, University of Education, Lahore, Pakistan*

Abstract This study was designed to prepare the sugarcane bagasse (SB) composite with polyaniline (PAn), polypyrrole (Ppy) and sodium alginate (NaA) and employed as an adsorbent for the adsorptive removal of herbicide (2,4-dicholorophenoxyacetic acid, 2,4-D). Fabricated composites were characterized by SEM and FTIR techniques. The affecting variables, i.e., temperature, contact time, initial herbicide concentration, medium pH and adsorbent dose were studied in batch mode. Different isotherms were employed on the adsorption data and the maximum adsorption capacity of SB was recorded to be 77.75 mg/g at pH 3.0, 150 mg/L 2,4-D initial concentration at 30 °C. The models (pseudo-second-order and Freundlich) best explained the adsorption experimental data with R^2 values ≥ 0.90 and ≥ 0.96, respectively. The thermodynamics parameters (ΔG, ΔH, and ΔS) were computed and the herbicide adsorption onto the composites was an exothermic and spontaneous

---

process. Results revealed that sugarcane bagasse composites with PAn, Ppy, and NaA are efficient adsorbents, which could be used for the remediation of 2,4-D in the effluents.

1. Introduction

To date, the contamination of toxic pollutants with water reservoirs is a worldwide issue, which is becoming more severe with the passage of time. Industrialization, urbanization, and agriculture are the main sectors responsible for water contamination and pollution (Aksu and Kabasakal 2004, Lammini et al., 2022, Laonapakul et al., 2022). Various strategies have been employed for the treatment of contamination to avoid the pollution issues with toxic chemical agents. Among wastewater treatment techniques, adsorption offers various advantages, i.e., economical, low cost, adsorbent available in abundance, high efficiency, and eco-benign nature (Awual et al., 2020, Awual et al., 2020, Şenol et al., 2022, Şimşek et al., 2022).

The 2,4-D is applied to manage broad leave herbs in the agriculture sector. It is carcinogenic, mutagenic, and induces a negative impact on the endocrine gland in living organisms. The 2,4-D is commonly found in the soil and groundwater agricultural areas, which is a serious hazard to the ecosystem. To avoid the negative impact, the 2,4-D need to be remediated before being water discharged into water bodies (Aksu and Kabasakal 2004, Salman and Al-Saad 2012, Evy Alice Abigail and Chidambaram 2016, Zhang and Han 2022). Therefore, the remediation of this pesticide from aqueous media is of particular significance. Different techniques, i.e., coagulation, biodegradation, flocculation, electrochemical oxidation, photocatalytic degradation, photodegradation, ozonation, adsorption using different adsorbents have been used for the remediation of pollutants (Sayed 2015, Daij et al., 2017, Minas et al., 2017, Awual 2019, Awual et al., 2019, Abbas et al., 2021, Jalal et al., 2021, Zeshan et al., 2022). Among these techniques, adsorption using advanced materials (modified biomasses and composites) offers a higher capability for the sequestration of pollutants from wastewater (Awual 2015, Angın and Güneş 2021, Awwad et al., 2021, Boumya et al., 2021).

The low-cost adsorbents are combined to prepare the composites and the composite/modified adsorbent offers additional advantages of higher cation exchange capability, enhanced mechanical strength, specific pore size and surface area, high stability, recycling, reusability, etc. These features enable the composite material to adsorb a higher concentration of adsorbate versus an un-modified counterpart (Awual 2019, Zhang and Han 2022). Literature survey based on comparative analysis of biosorption capacities of different adsorbents for model pollutant has been added in Table 1. The remediation of pesticides from wastewater using the composite materials have not been studied extensively. The composite materials are also cost-effective due to the usage of sugarcane bagasse, a waste material.

Keeping in view the above-mentioned facts, in the present investigation, sugarcane bagasse composites were prepared with PAn, Ppy, and NaA. The composites were employed for the adsorption of 2,4-D. The affecting variables, i.e., temperature, composite dose, contact time, pH, and herbicide initial concentration effect on removal efficiency were studied. The isotherms, kinetics, and thermodynamics modeling were performed to appraise the herbicide adsorption nature onto the composites.

2. Material and methods

2.1. Chemical and reagents

The hydrochloric acid (37 %), aniline (99.8 %), CH_3OH (97 %), pyrrole (98 %), CH_3COOH (99.01 %), ammonium persulfate (98 %), sulfuric acid (98 %), potassium nitrate (99.0 %), sodium chloride (97.5 %), Calcium chloride (98.0 %) and aluminium chloride (98 %) of Sigma-Aldrich origin were used during the study.

2.2. Sample collection

The herbicide was purchased from Ali Akbar Group, Lahore, Pakistan. Different waste biomasses, i.e., BH (barley husk), SD (saw dust), SB (sugarcane bagasse), MD (mustard), PH (peanut husk), RH (rice husk), CT (citrus) and eucalyptus (ET), were collected from crop fields, Faisalabad, Pakistan. These samples were sliced into small pieces, cleaned with water, dried in the air and then, finally, at 60 °C in oven overnight. The dried biomasses were grinded and passed through OCT-DIGITAL4527-01 siever. For the removal of color, biomasses were treated with formaldehyde. Biomass (10 g) was added in 5 mL of formaldehyde and 100 mL of 0.1 M H_2SO_4 and stirred at 50 ^{0}C for 36 h (Yadamari et al., 2011). Then, filtration was done for biomass collection, which was

Table 1 Comparative analysis of biosorption capacities of SB and its composite for 2,4-D with literature.

Adsorbent	pH	Time (min)	Temp (K)	Adsorption capacity	Concentration (mg/L)	Adsorbent dose (g)	Reference
Rice husk	5	60	303	96.87 %	–	–	(Evy Alice Abigail and Chidambaram 2016)
Granular carbon	2	–	328	520 mg/g	600	–	(Aksu and Kabasakal 2004)
zirconium elemental organic framework	3	–	303	652 mg/g	–	0.008	(Zhang and Han 2022)
orange pulp activated carbon	6.22			71.94 mg/g	300	0.3	(Angın and Güneş 2021)
Date Seeds Activated Carbon	–	–	303	139.7 mg/g	300	–	(Salman and Al-Saad 2012)
PPY-SB	4	120	303	21.01 mg/g	25	0.05	Present study
SB	4	120	303	17.75 mg/g	25	0.05	Present study
PAn-SB	4	120	303	16.85 mg/g	25	0.05	Present study

rinsed water, dried, ground, sieved and homogeneous particle size of 25 mm was collected.

2.3. Preparation of biocomposites

For polyaniline (PAn) biocomposite, aniline (5 mL) was assorted with hydrochloric acid (1 M) and kept in ice bath. Then, 0.5 M (NH$_4$)$_2$S$_2$O$_8$ was mixed slowly, stirred for 2 h, kept overnight, filtered and rinsed with water and methanol (Gupta et al., 2004) and a PAn of dark green color was obtained. In the next step, EB (Emeraldine-base) PAn was prepared. For this, a 5 g of PAn was poured NaOH (100 mL, 0.5 M), stirred it for 3 h, filtered, dried and used for composite preparation. Then, formic acid (50 mL) was mixed with 0.5 g of the EB form of PAn and stirred for 15 min. Then, 5 g of sugarcane bagasse (SB) was added and stirred for 3 h and dried at 60 ^{0}C for 4 h. For polypyrrole (Ppy) composite preparation, the pyrrole (100 mL) was assorted with 3 g of SB and kept for 24 h. Then, 0.5 M FeCl$_3$ was mixed in it slowly, kept overnight, filtered and cleaned with plenty of water and then, with methanol and dried at 60 ^{0}C for 4 h (Palanisamy et al., 2012). For NaA-SB, 2 g of sodium alginate was mixed in hot water, stirred till a slurry is appeared, cooled down to room temperature. Then, SB (1 g) was mixed in the slurry and homogenized the mixture by stirring. The slurry was dropped in in CaCl$_2$ (0.1 M) and beads thus formed was stored in 0.05 M CaCl$_2$ at 4 ^{0}C (Bayramoglu et al., 2002). Reaction mechanism for PAn-SB, Ppy-SB and NaA-SB synthesis are shown in Figs. 1-3, respectively.

2.4. Biosorption studies

For 2,4-D biosorption, initial concentration of 2,4-D, temperature, pH and composite dose were studied in batch mode. For pH adjustment, HCl/NaOH (0.1 M) was used. Erlenmeyer flask (250 mL) was used for batch experiments and the sorbent
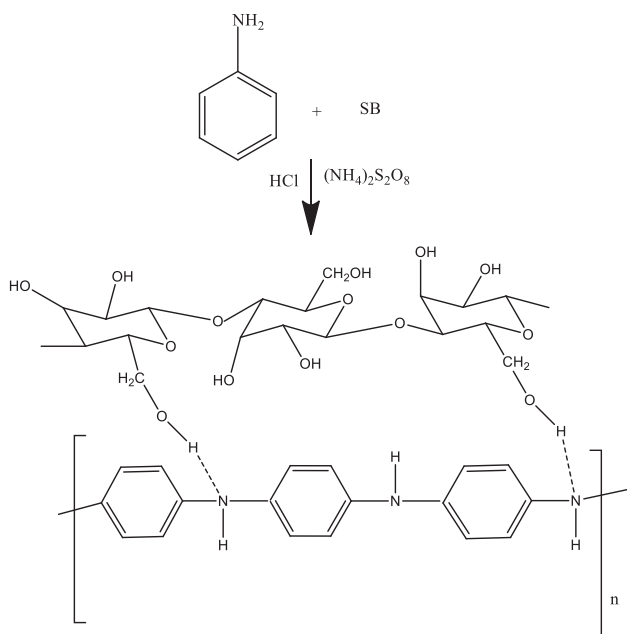

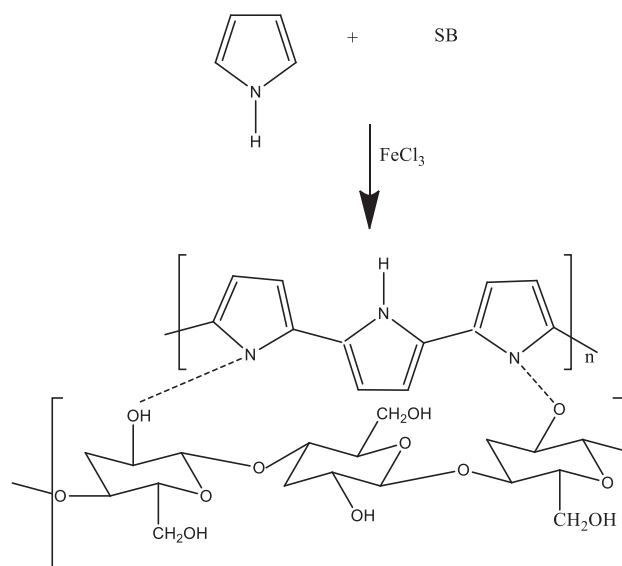**Fig. 1** PAn-SB composite synthesis scheme.

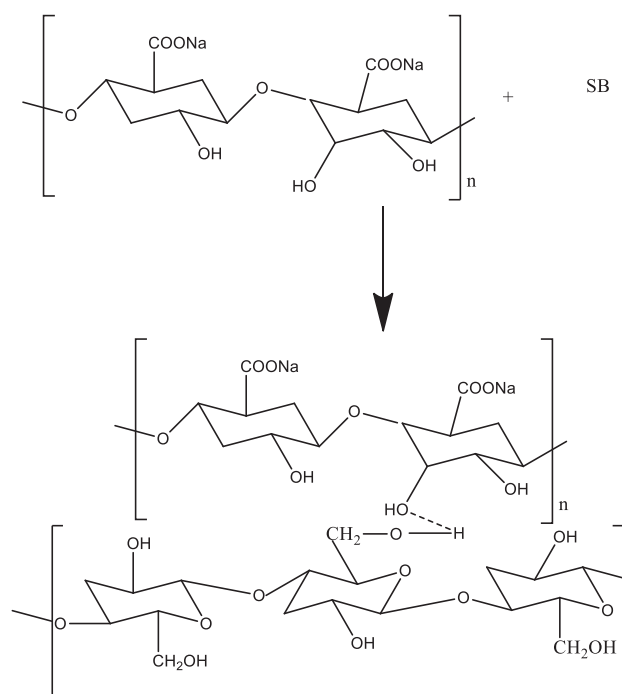
Fig. 2 Ppy-SB composite synthesis scheme.

Fig. 3 NaA-SB composite synthesis scheme.

dose (0.03–0.30 g), agitation time (5–120 min), 2,4-D initial concentration (10–200 mg/L), 303–333 K and pH (2–7) were studied for the 2,4-D adsorption using all composites. After adsorption, the adsorbent was separated by filtration, the 2,4-D concentration (residual) was estimated at 227 nm and the adsorption efficiency (q_e) was appraised as per Eq. (1) (Where, q = adsorption capacity; C_i = initial conc. of 2,4-D; C_e = equilibrium conc.; V = volume in dm^3 and W = mass of biomass in g).

$$q_e = \frac{(C_o - C_e) \times V}{W} \tag{1}$$

3. Results and discussion

3.1. Composites properties

FT-IR technique was utilized for the identification of active moieties on the exterior of the composites (Salem and Awwad 2022). Adsorption is a surface phenomenon and functional groups play vital role in this regard. FTIR analysis of SB and its composites (loaded and unloaded) is shown Fig. 4. A broad peak in unloaded SB appears at 2700–3500 cm^{-1} due to presence of cellulose and hemicellulose. Peaks between 1580 cm^{-1} and 1700 cm^{-1} is due to the presence of carboxylic group in lignin and hemicellulose. While a peak at 1060 cm^{-1} represents the C—O stretching vibration in cellulose. The peaks in loaded spectra have shifted towards shorter wavelength and are less intense than unloaded SB. This shifting is due to involvement of functional groups in adsorption.

FTIR analysis Ppy-SB composite (unloaded and loaded) is shown in Fig. 4. Appearance and disappearance of peaks are due to the involvement of functional groups in adsorption process. In unloaded spectra peak around 1680 cm^{-1} was correlated with C=O vibrations. A band at 1550 cm^{-1} is due C—N stretching vibration of pyrrole ring. An intense peak at 1180 cm^{-1} shows the C—N in plane deformation. While in loaded spectra, peak for C=O stretching vibrations is less intense and peaks for C—N stretching and C—N in plane deformation shift to1530 cm^{-1} and 1160 cm^{-1} respectively, which revealed the participation of the respective group in the sorption of 2, 4-D.

In PAn-SB spectra a broad peak between 2800 cm^{-1} and 3300 cm^{-1} is due to –OH, –COOH functional groups of cellulose, hemicellulose and lignin which are basic components of sugarcane bagasse. At 1550 cm^{-1} small peak represents the

N—H deformation of secondary amine. Small peaks of C—N stretching between 1300 cm^{-1} and 1400 cm^{-1} depicts that secondary aromatic amines are present. Around 1070 cm^{-1} a very intense peak is due to stretching of C—O of –OCH$_3$ which is present in lignin. In loaded spectra these peaks are less broad and short, which revealed their interaction with 2,4-D.

In NaA-SB spectra medium broad peak in the region of 2950 cm^{-1} – 3700 cm^{-1} shows the hydrogen bonding due to –OH group and N—H bond in biomass. The broadness of the peak depicts that the –OH bond belongs to carboxylic group. Sharp peak around 1600 cm^{-1} is due to C=O vibration. two intense peaks of C—O stretching at 1060 cm^{-1} and 1150 cm^{-1} is due to the presence of ether group in sodium alginate. while in the case of loaded spectra, all the peaks are at same position but have lower intensities, which indicates the participation of respective groups for 2,4-D adsorption on to the adsorbent (Maqbool et al., 2020).

The SEM is employed for the appraisal of morphology of the composites (Shammout and Awwad 2021, Naseer et al., 2022). SEM images of unloaded biomass and biocomposites of SB, Ppy-SB, PAn-SB and NaA-SB are presented in Fig. 5. Fig. 5(A) shows that SB has fibrous structure having smooth surface. Fig. 5(B) shows that the surface of Ppy-SB composite is uneven and porous. Fig. 5(C) shows that the PAn-SB composite has irregular shape with different pore sizes while NaA-SB has bead like structure as shown in Fig. 5(D). The Results indicate that the adsorption capacity of the biomass and biocomposites are in the order of Ppy-SB > SB > PAn-SB > N aA-SB. Adsorption capacity is directly related to porosity. More the pores, higher will be the adsorption efficiency of composite. In this study, Ppy-SB has more porous structure as compare to others, hence it is more efficient for the sequestration of 2,4-D and NaA-SB is least efficient. SEM of loaded
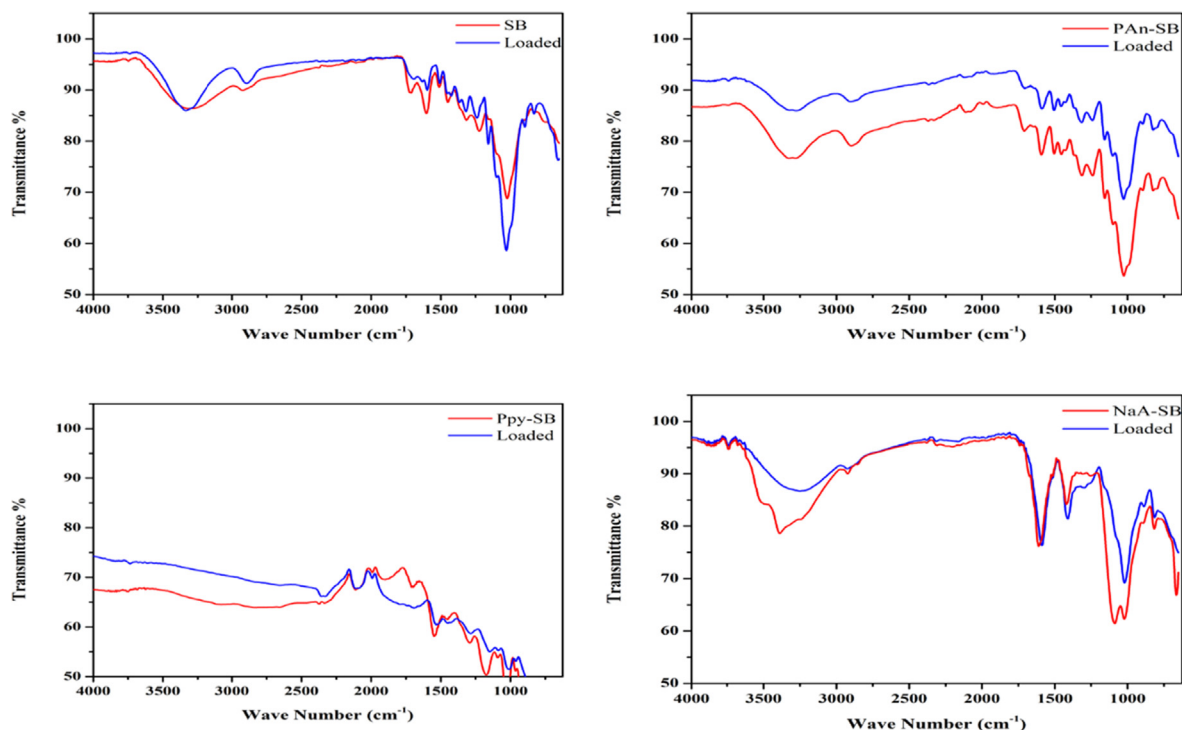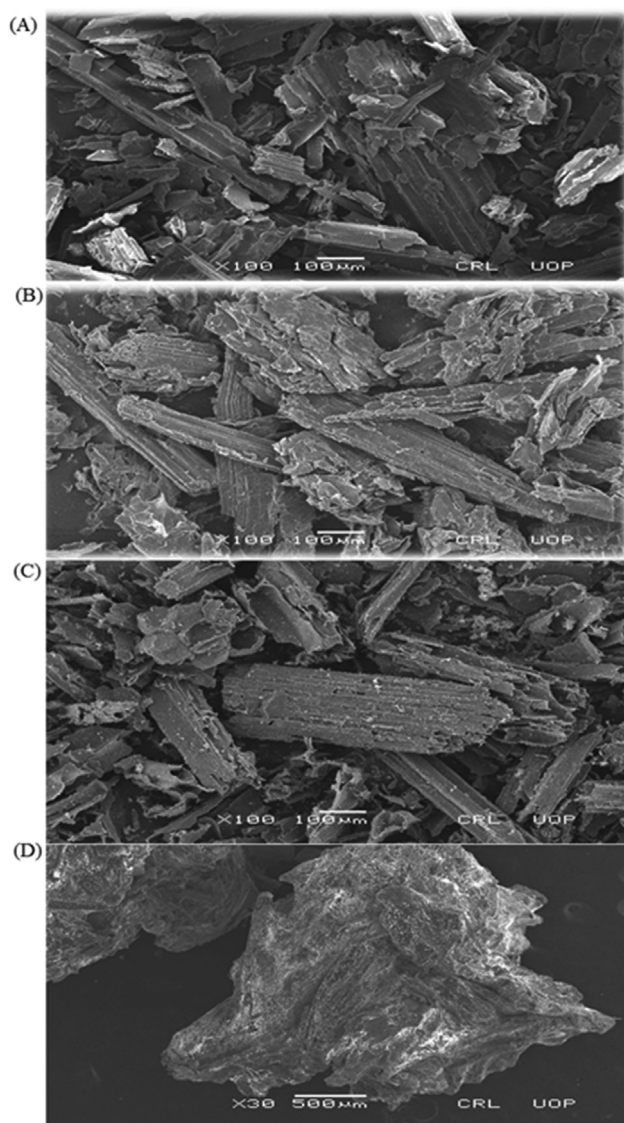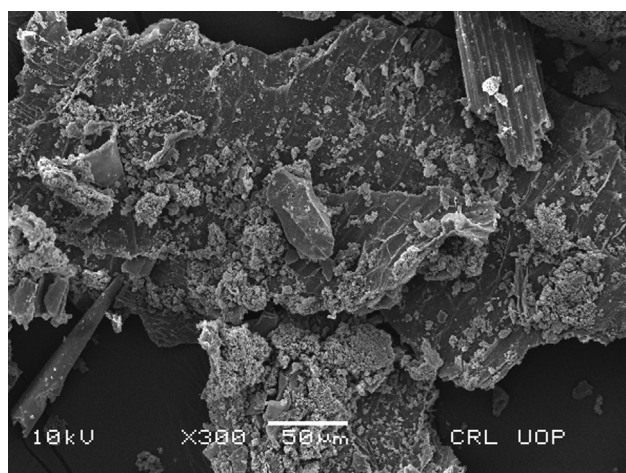

Fig. 4   FT-IR spectra of composites before and after adsorption.

Fig. 5 SEM images; (A) SB, (B) PAn-SB, (C) Ppy-SB and (D) NaA-SB used for the adsorption of 2,4-D.

Fig. 6 SEM image of Ppy-SB loaded with 2,4-D.

PPY-SB is also presents in Fig. 6, which revealed a significant change in the surface morphology of the adsorbent before and after the adsorption of 2,4-D.

3.2. Screening, point of zero charge and reaction mechanism

Initially, adsorption of 2,4-D was performed using different waste biomasses such as mustard, sugarcane bagasse, citrus, peanut husk, eucalyptus, rice husk, saw dust and barley husk and output is depicted in Fig. 7. SB showed higher efficiency for the adsorption (6.33 mg/g) of 2,4-D. The surface properties of different adsorbents might be the reason for this trend and results are in line with reported studies, i.e., the adsorption potential of different biomasses like cotton sticks, peanut hull, sugarcane bagasse, and rice bran was investigated for the sequestration of malachite green dye and rice bran was efficient (Bhatti et al., 2017). The charge on the biomass surface become zero at the point of zero charge. The nature of charge is helpful in the determination of cations and anions adsorption possibility, i.e., anion adsorption is favorable at pH < pH_{pzc}, and adsorption of cation is significant when pH > pH_{pzc} (Noreen et al., 2022). At pH < pH_{pzc}, the composite surface bears positive charge, which shows strong electrostatic forces for anionic molecules and pH > pH_{pzc} is an indication that composite surface has negative charge, which allows cationic species to be adsorbed on the surface efficiently. Potassium nitrate (KNO_3) (0.1 M) was used to deduce the pH_{pzc} and the response is shown in Fig. 8 and pH_{pzc} was found to be 4.0 in the case of SB. The adsorption mechanism is shown in Fig. 9. Mechanism provides evidences regarding the attachment of anionic moiety over positively charged adsorbent surface as per the pH_{pzc} analysis of the adsorbents.

3.3. Effect of process variables on adsorption

3.3.1. Effect of pH

The pH of a system is one of paramount variables in the adsorption process and interaction of adsorbate with adsorbent depends on the chemistry of solution (Awual 2019). By changing the pH, the interaction between the adsorbent and 2,4-D was changed, which was studied in the range of 2–7 pH (Fig. 10). The 2,4-D is a weak acid and present in anionic form. On the basis of point of zero charge analysis, it was proved that pH < 4 is favorable for efficient adsorption.
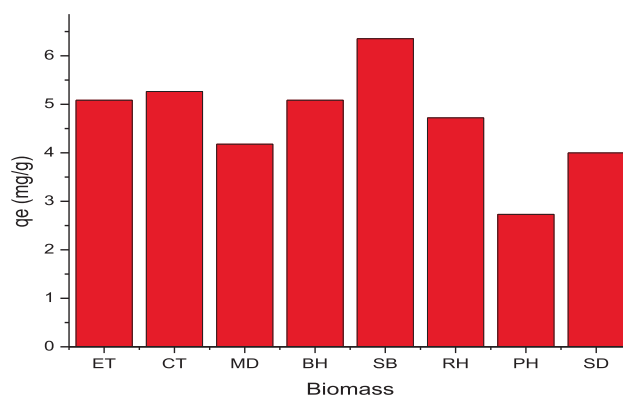
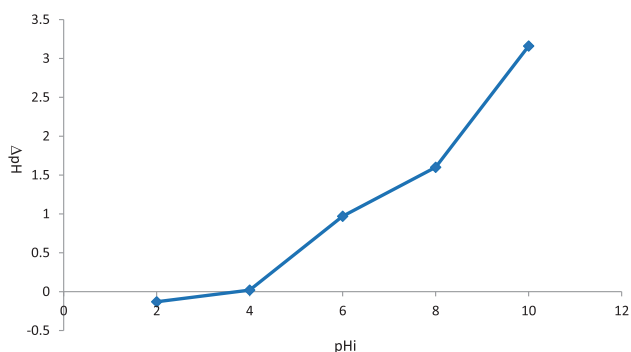Fig. 7 Adsorption capacities of different waste biomasses for 2,4-D.
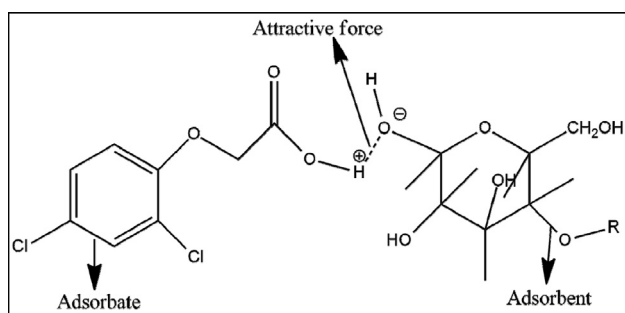
Fig. 8 Point of zero charge of on biomass.

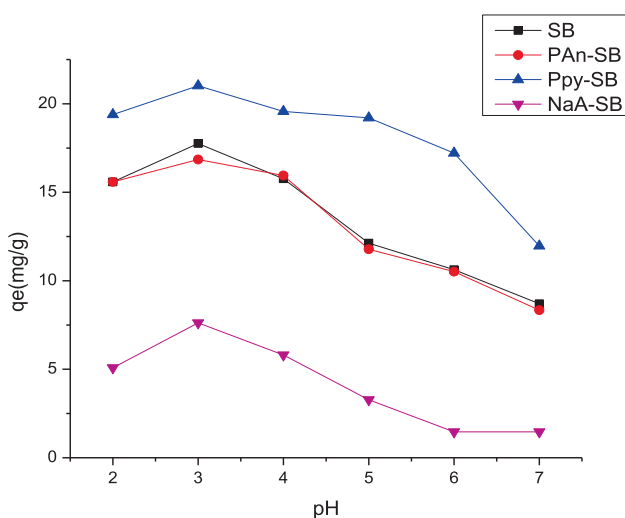**Fig. 9** Adsorption mechanism for the adsorption of 2,4-D onto the composite.

Fig. 10 Effect of pH on the adsorption of 2,4-D using prepared composites.

The optimum pH for SB and biocomposites was 3 and the biosorption capacities for SB, PAn-SB, Ppy-SB and NaA-SB were 17.75, 16.85, 21.01 and 7.6 (mg/g), respectively at pH 3. This study is in line with a silica-based composite employed as an adsorbent, which showed the optimum pH was 1.5 (Awual et al., 2020).

3.3.2. Composite dose effect

The dose of the composite has substantial impact on adsorption since adsorption depends on the binding moieties on the

composite surface and vice versa. The adsorbent dose effect was investigated from 0.05 to 0.3 g and responses are depicted in Fig. 11. The composite dose offers a promising impact on the adsorption efficiency and maximum 2,4-D removal was observed when 0.05 g composite dose was used. The biosorption values at optimum dosage (0.05 g/25 mL) for SB, PAn-SB, Ppy-SB and NaA-SB were 17.75, 16.85, 21.01 and 7.6 (mg/g), respectively. As the composite dose was augmented, the 2,4-D sequestration was declined linearly. It might be due to overlapping of adsorbent particle, which reduced the binding moieties at higher composite doses. Also, the availability of active binding sites may decrease at higher adsorbent dose due to aggregates form of the adsorbent (Maqbool et al., 2021).

3.3.3. Effect of contact time

Contact time is also an adsorption affecting variable, which was studied from 5 to 120 min for the 2,4-D sequestration on to composites (Awwad et al., 2021) and output is depicted in Fig. 12. It was observed that the 2,4-D sequestration on to composites was very fast at initial stages, which slowed down and finally, equilibrium was reached. Experimental study showed that the optimum time was 120 min for the prepared composites. Initially, the vacant sites on the adsorbents surface were available to bind the 2,4-D ions; hence adsorption was fast initially. As the contact time proceeded, the active sites became saturated and resultantly, the adsorption capacity slowed down and finally, becomes constant due to unavailability of active sites. The current observations corelates well with reported studies that the composite perform fast versus native biomasses. It has been reported that the removal of pollutants on composites was fast in comparison to native biomasses (Ishtiaq et al., 2020). Contac time effect was studied using imidacloprid as an adsorbate and PH and its composites with polyaniline, polypyrrole and sodium alginate as an adsorbent.it was observed that biosorption rate first increases and then become constant due to the locking up of all available sites (Maqbool et al., 2021).
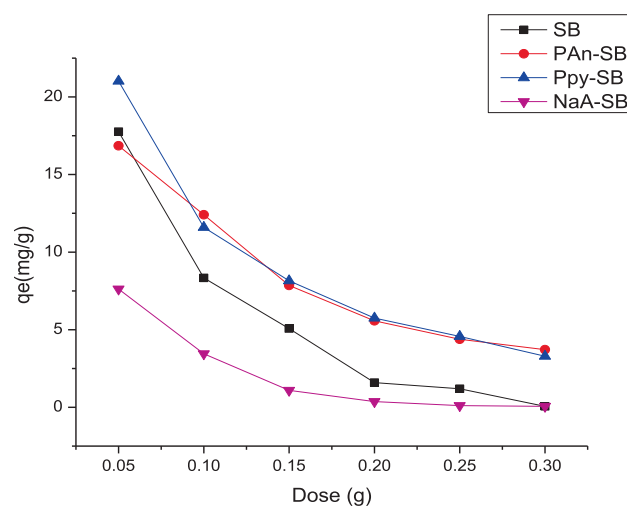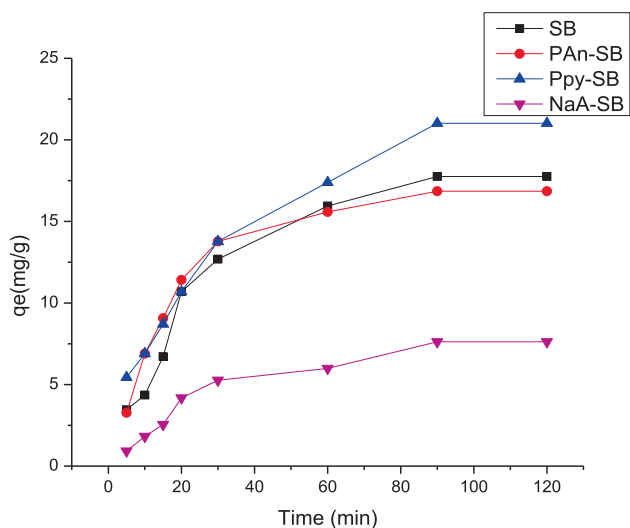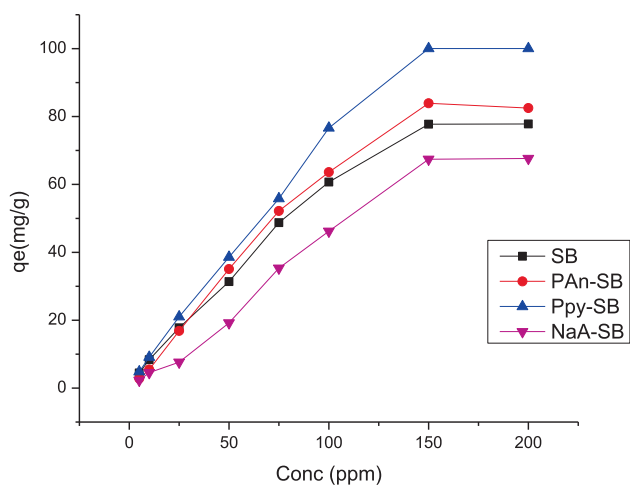

Fig. 11 Effect of adsorbent dose on the adsorption of 2,4-D using prepared composites.

Fig. 12 Effect of contact time on the adsorption of 2,4-D using prepared composites.

3.3.4. 2,4-D concentration and temperature effect

The 2,4-D concentration also affects the process of adsorption due to mass transfer and gradient factors. The effect of 2,4-D concentration was appraised in 5 to 200 mg/L range and response thus observed is shown in Fig. 13. As the initial 2,4-D concentration was increased, the sequestration efficiency was also increased that was increased up to 150 m/L and later, it become steady. The 2,4-D sequestration was recorded to be in 4.46–77.82 mg/g range for 5–200 g/L 2,4-D concentration. The adsorption was enhanced with 2,4-D concentration because the binding sites became saturated and beyond certain concentration, the adsorption became constant since all available bindings sites were occupied (Ishtiaq et al., 2020). Also, the collisions between binding sites and 2,4-D are higher as a function of 2,4-D concentration. Temperature also has significant affect the adsorption phenomena, which was studied from 303 to 333 K and responses thus observed, are shown in Fig. 14. With temperature, the rate of adsorption was

decreased, which revealed that the process of 2,4-D removal was exothermic for all composites. This effect can also be explained on the basis of adsorptive forces, which may become weak at high temperature. The deactivation of active site might also be the reason of decreased adsorption at elevated temperature[42, 43].

3.4. Thermodynamic study

Thermodynamic study is useful to check the feasibility of the adsorption process. The ΔH, ΔG and ΔS were calculated using relation shown in Eqs. 2–3. At lower temperature, the values of ΔG for SB, PAn-SB and PPY-SB were negative, which confirms the spontaneity of the 2,4-D sequestration on to the composites (Table 2) and at higher temperature. the ΔG values were positive for SB, PAn-SB and Ppy-SB composites. The negative value of enthalpy changes for SB and its biocomposites confirms that the reaction is exothermic in nature. The NaA-SB composite behavior was different and ΔG was found to be positive for NaA-SB, while ΔG and ΔS values were negative.

$$\Delta G = \Delta H - T\Delta S \qquad (2)$$

$$\ln K_d = \frac{\Delta S}{R} - \frac{\Delta H}{RT} \qquad (3)$$

Where, ΔG = change in free energy, R = gas constant, K_d = equilibrium constant, T = temperature, ΔH = change in enthalpy and ΔS = change in entropy,

3.5. Kinetics study

The pseudo first order (Eq. (4)), pseudo second order (Eq. (5)) and intraparticle diffusion models was employed on the 2,4-D sequestration data (Ho and McKay 1999, Ho et al., 2000). The kinetics applicability is based on R^2 value and relation between q_{cal} and q_{exp}. Kinetics data is depicted in Table 3.

$$\log (q_e - q_t) = log q_e - k_i t/2.303 \qquad (4)$$

Where, q_e, q_t, K_1 and t are representing the adsorption capacity, adsorption at time t, rate constant and contact time, respectively. Pseudo second order kinetic model refers to the chemisorption process. The relation for pseudo second order is depicted in Eq. (5).

Fig. 13 Effect of 2,4-D initial concentration on the adsorption of 2,4-D using prepared composites.
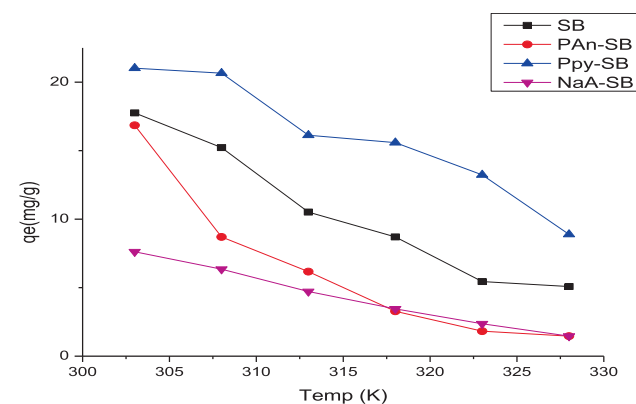
Fig. 14 Effect of temperature on the adsorption of 2,4-D using prepared composites.

Table 2 Thermodynamic parameters for the adsorption of 2,4-D using prepared adsorbents.

	SB			PAn-SB		
Temperature (K)	ΔG kJ/mol	ΔH kJ/mol	ΔS J/mol.K	ΔG kJ/mol	2206H kJ/mol	ΔS J/mol.K
303	−2.26	−79.57	−255.489	−1.826	−114.58	−374.88
308	−1.13			1.6133		
313	0.84			2.914		
318	1.67			5.025		
323	3.45			6.86		
333	3.73			7.62		
	Ppy-SB			NaA-SB		
303	−4.19	−74.13	−229.8	2.09	−64.89	−219.99
308	−3.99			2.77		
313	−1.56			3.81		
318	−1.33			4.86		
323	−0.309			6.09		
333	1.63			7.62		

Table 3 Kinetics parameters for the adsorption of 2,4-D using prepared adsorbents.

Kinetic models	SB	PAn-SB	Ppy-SB	NaA-SB
Pseudo first order				
K_1 (L/min)	0.025	0.023	0.025	0.016
q_e exp (mg/g)	17.75	16.84	21.01	7.6
q_e cal (mg/g)	13.46	9.66	17.22	5.65
R^2	0.92	0.85	0.96	0.87
Pseudo second order				
K_2 (g/mg min)	0.0014	0.003	0.0014	0.0020
q_e exp (mg/g)	17.75	16.84	21.01	7.6
q_e cal (mg/g)	23.26	20	26.32	10.87
R^2	0.97	0.99	0.99	0.96
Intraparticle diffusion				
K_{pi} (mg/g min$^{1/2}$)	1.76	1.46	1.93	0.79
C_i	0.76	3.08	1.67	− 0.158
R^2	0.90	0.84	0.97	0.92

$$\frac{t}{q_t} = \frac{1}{k_2 q_e^2} + \frac{t}{q_e} \tag{5}$$

Where, t, k_2, q_e and q_t are contact time, rate constant, adsorption capacity and adsorption at time t, respectively.

The kinetics data thus calculated is shown in Table 3 and the R^2 values for SB, PAn-SB, Ppy-SB and NaA-SB were recorded to be 0.97, 0.99, 0.99 and 0.94, respectively for pseudo second order, which revealed that the pseudo second fitted well to the 2,4-D adsorptive behavior on to composites. Fitness of the model can also be explained on the basis of compatibility in q_e and q_{cal}. As in case of SB values are 17.75 and 23.26 (mg/g) for q_e and q_{cal}, respectively are in good agreement. The same case is with other three composites which confirm the 2,4-D sequestration data followed the pseudo second order kinetics. This observation also proves that the adsorption of 2,4-D adsorption on to composites was a chemisorption process. The trend thus observed in this study also corelates well with reported studies that composites of biopolymers followed pseudo second order kinetic model, i.e., it was observed that the adsorption of malachite green on to the composites of rice bran with polyaniline, polypyrrole, starch, aniline and chitosan followed pseudo second order kinetics model (Bhatti et al., 2017). For pseudo first order, the value of R^2 for SB, PAn-SB, Ppy-SB and NaA-SB were 0.918, 0.847, 0.962 and 0.886, respectively, which are lower than the pseudo second order, hence, pseudo second order fitted well to the 2,4-D data, which is an indication of chemisorption process (Şenol and Şimşek 2022).

The adsorption of adsorbate from solution to the adsorbent took place in different steps, i.e., in single step or in different steps. These steps may be the film formation, intraparticle or combination of both and for this, relation is shown in Eq. (6).

$$q_t = k_{pi} t^{1/2} + C_i \tag{6}$$

Where, q_t, C_i, and K_p are adsorption capacity, constant (boundry layer thickness) and rate constant. The values of R^2 for intraparticle diffusion model were recorded to 0.90, 0.84, 0.97 and 0.92 for SB, PAn-SB, Ppy-SB and NaA-SB, respectively. Plots constructed for 2,4-D adsorption on to composites was not passed from a origin, which is an indication that the diffusion was not the rate-limiting step.

3.6. Isotherms modeling

Langmuir isotherm deals with the formation of monolayer of the adsorbate on the composite surface (Langmuir 1918). The Langmuir model is presented in Eq. (7).

$$\frac{C_e}{q_e} = \frac{1}{q_m . K_L} + \frac{C_e}{q_m} \tag{7}$$

Where, q_m = maximum adsorption capacity and Ce = equilibrium concentration. R_L is an important factor of Langmuir model, which is computable using in Eq. (8).

$$R_L = \frac{1}{1 + bC_0} \tag{8}$$

Where, R_L is the separation factor, b is a constant, C_0 is the 2,4-D initial concentration. R_L is used to check whether the process is favorable or not, if ($0 < R_L < 1$) then, the process is favorable, unfavorable ($R_L > 1$), irreversible ($R_L = 0$) or linear ($R_L = 1$). The values of R^2 were found to be 0.959, 0.598,

0.965 and 0.053 for SB, PAn-SB, Ppy-SB and NaA-SB, respectively (Table 4), which indicates that Langmuir model fitted well to the SB and Ppy-SB composite.

The Freundlich isotherm deals with the multilayer adsorption of adsorbate molecules on the surface of adsorbent and also assume the heterogeneous surface of adsorbent and relation is shown in Eq. (9) (Freundlich 1906).

$$logq_e = logk_f + (1/n)logC_e \qquad (9)$$

Where, q_e is the adsorbed amount on adsorbent surface and measured (mg/g). n and K_F are the Freundlich constants. K_F represents the adsorption capacity, while n is useful to evaluate the type of assorption as; if n = 1 (linear), n < 1 (chemical process) and n > 1 (favorable). The values of K_F, n and R^2 for SB, PAn-SB, Ppy-SB and NaA-SB are presented in Table 4. The data showed that Freundlich isotherm model explained well the 2,4-D removal using composite and the value of n > 1 indicates that the process was favorable for the adsorption of 2,4-D on to composites. Temkin model deals with the binding energies on the binding sites of the adsorbent (Temkin 1940). The straight-line equation of Temkin isotherm is shown in Eq. (10).

$$q_e = BlnA + BlnC_e \qquad (10)$$

Where, B = RT/b, A is the constant and Temkin constant is b, while R is a gas constant. The value of A, B and R^2 can be determined by plotting a graph among q_e and lnC_e, where slope gives the value of B and the value of A can be determined from intercept. Temkin isotherm data for SB and composites is shown in Table 4 and it was observed that this model fitted well to the PAn-SB adsorption data. The Harkins–Jura isotherm deals with multilayered adsorption and heterogeneous pore distribution (Harkins and Jura 1944) (Eq. (11)).

$$1/q_e^2 = B/A - |1/A|logC_e \qquad (11)$$

Where, A and B are the constants. The value of A and B is computed from plot of $logCe$ versus $1/qe^2$. The Harkins Jura isotherm data is shown in Table 4 and it was observed that this model to unable to explain the 2,4-D on to composites. Doubinin-Radushkevich isotherm was also applied and the straight line form of D-R model is shown in Eq. (12) (Dubinin and Raduskhevich 1947).

$$lnq_e = lnq_m - \beta\varepsilon^2 \qquad (12)$$

Where, β is a constant, which represents adsorption energy and ε represents the Polanyi potential. Polanyi potential can be calculated using Eq. (13) and mean free energy is computed using Eq. (14).

$$\varepsilon = RTln(1 + \frac{1}{C_e}) \qquad (13)$$
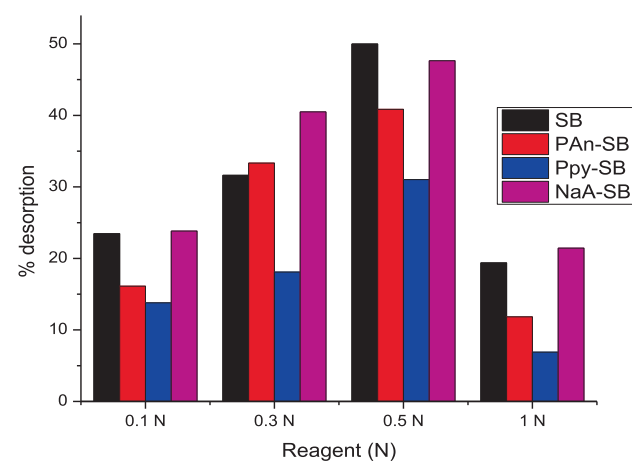
$$E = 1/(2\beta)^{1/2} \qquad (14)$$

The D-R model indicates that the model is not fitted to the 2,4-D sequestration on to composites. The values of R^2 were 0.637, 0.734, 0.596 and 0.612 for SB, PAn-SB, Ppy-SB and NaA-SB, respectively. Also, the q_e calculated and q_e experimental did not match with each other.

3.7. Desorption study

Discarding of adsorbent waste after removal is a drawback of the adsorption technique, which cause secondary pollution issue. Desorption study is also useful to recover the adsorbate. The loaded composite was filtered, dried and stirred by mixing with eluting agent for 120 min. For desorption purpose, 0.1–1.0 N NaOH was used as an eluting agent. It was observed that as the eluting agent concentration was increased, the 2,4-D sequestration from the composites was also increased and beyond this concentration, the 2,4-D desorption was decreased (Fig. 15) and these observation corelates well with reported studies that the desorption and extent of desorption depends upon the eluting agent (Ishtiaq et al., 2020). A summary for adsorption efficiencies of 2,4-D from using composites is depicted in Table 5 and the findings revealed that the sugar-

Table 4 Equilibrium modeling data for the adsorption of 2,4-D using prepared adsorbents.

Isotherms	SB	PAn-SB	Ppy-SB	NaA-SB
Langmuir				
q_m cal (mg/g)	100	166.67	125	500
q_m exp (mg/g)	77.75	83.91	100.03	67.43
b	0.042	0.012	0.068	0.0015
R_L	0.107	0.293	0.068	0.772
R^2	0.959	0.598	0.965	0.053
Freundlich				
K_F	6.37	1.96	11.04	0.83
n	1.76	1.101	1.88	1.05
R^2	0.98	0.908	0.98	0.96
Temkin				
A	1.143	0.354	2.55	0.215
B	14.94	23.68	16.84	18.36
R^2	0.885	0.955	0.852	0.817
Harkins-Jura				
A	55.56	18.18	76.92	10.64
B	1.61	1.6	1.46	1.76
R^2	0.703	0.543	0.73	0.68
Doubinin-Radushkevich				
q_m (mg/g)β (mol²kJ⁻²)E (kJmol⁻¹)	40.69 4.00E-07	45.88 4.00E-06	48.18 1.00E-07	29.37 5.00E-06
R^2	1.118 0.637	0.354 0.734	2.236 0.596	0.316 0.612

Fig. 15 Desorption of 2,4-D from SB, PAn-SB, Ppy-SB and NaA-SB using NaOH as eluting agent.

Table 5 Optimum conditions and adsorption efficiency of 2,4-D adsorption analysis for the prepared adsorbents.

Adsorbent	pH	Adsorbent dose (g)	Contact time (min)	Initial conc. (ppm)	Temp (K)	q_e (mg/g)
SB	3	0.05	90	150	303	17.75
PAn-SB	3	0.05	90	150	303	16.84
PPy-SB	3	0.05	90	150	303	21.01
NaA-SB	3	0.05	90	150	303	7.6

cane bagasse composite with polyaniline, polypyrrole and sodium alginate showed promising affinity for 2,4-D. The water bodies contamination is one of major issues due to anthropogenic mixing of pollutants in water bodies. For the enhancement of yield of agriculture crops, herbicides and pesticides are used extensively, which in turn polluting the water resource (Awual et al., 2017, Şimşek et al., 2017, Awual 2019, Awual 2019, Sasmaz et al., 2020, Elsherif et al., 2021, Sasmaz et al., 2021, Sasmaz et al., 2021, Awwad and Amer 2022), which need to be undertaken on priority basis. The development of advanced functional materials based on agricultural waste might be useful for the preparation of adsorbents for effective adsorptive removal of herbicides. In this regard, the composite of cellulosic materials with biomolecules proved to be one of potential class of the materials as an adsorbent.

4. Conclusions

Native SB and its biocomposites were fabricated and employed for the sequestration of 2,4-D from wastewater. Effect of various process variables were studied and optimum conditions were pH 3, composite dose 0.05 g/50 mL, 303 K and 90 min contact time for all four types of biosorbents. The order of adsorption capacity was found as Ppy-SB > SB > PAn-SB > NaA-SB. The 2,4-D adsorption followed the pseudo second order and Freundlich isotherm models. Thermodynamic study indicated the exothermic and spontaneous nature of 2,4-D removal using composites. The composites of cellulosic sugarcane bagasse with PAn, Ppy and NaA are efficient and could be used for the adsorptive removal of 2,4-D from effluents and also these are extendable for other herbicides remediation.

Declaration of Competing Interest

The authors declare that they have no known competing financial interests or personal relationships that could have appeared to influence the work reported in this paper.

References

Abbas, N., Butt, M.T., Ahmad, M.M., et al, 2021. Phytoremediation potential of Typha latifolia and water hyacinth for removal of heavy metals from industrial wastewater. Chem. Int. 7, 103–111.

Aksu, Z., Kabasakal, E., 2004. Batch adsorption of 2,4-dichlorophenoxy-acetic acid (2,4-D) from aqueous solution by granular activated carbon. Sep. Purif. Technol. 35, 223–240.

Angın, D., Güneş, S., 2021. The usage of orange pulp activated carbon in the adsorption of 2, 4-dichlorophenoxy acetic acid from aqueous solutions. Int. J. Phytorem. 23, 436–444.

Awual, M.R., 2015. A novel facial composite adsorbent for enhanced copper(II) detection and removal from wastewater. Chem. Eng. J. 266, 368–375.

Awual, M.R., 2019. An efficient composite material for selective lead (II) monitoring and removal from wastewater. J. Environ. Chem. Eng. 7, 103087.

Awual, M.R., 2019. Efficient phosphate removal from water for controlling eutrophication using novel composite adsorbent. J. Cleaner Prod. 228, 1311–1319.

Awual, M.R., 2019c. A facile composite material for enhanced cadmium(II) ion capturing from wastewater. J. Environ. Chem. Eng. 7, 103378.

Awual, M.R., 2019d. Innovative composite material for efficient and highly selective Pb (II) ion capturing from wastewater. J. Mol. Liq. 284, 502–510.

Awual, M.R., Alharthi, N.H., Okamoto, Y., et al, 2017. Ligand field effect for Dysprosium(III) and Lutetium(III) adsorption and EXAFS coordination with novel composite nanomaterials. Chem. Eng. J. 320, 427–435.

Awual, M.R., Hasan, M.M., Islam, A., et al, 2019. Offering an innovative composited material for effective lead (II) monitoring and removal from polluted water. J. Cleaner Prod. 231, 214–223.

Awual, M.R., Hasan, M.M., Iqbal, J., et al, 2020. Naked-eye lead(II) capturing from contaminated water using innovative large-pore facial composite materials. Microchem. J. 154, 104585.

Awual, M.R., Hasan, M.M., Islam, A., et al, 2020. Optimization of an innovative composited material for effective monitoring and removal of cobalt(II) from wastewater. J. Mol. Liq. 298, 112035.

Awwad, A.M., Amer, M.A., 2022. Adsorption of Pb(II), Cd(II), and Cu(II) ions onto SiO_2/kaolinite/Fe_2O_3 composites: modeling and thermodynamics properties. Chem. Int. 8, 95–100.

Awwad, A.M., Salem, N.M., Amer, M.W., et al, 2021. Adsorptive removal of Pb (II) and Cd (II) ions from aqueous solution onto modified Hiswa iron-kaolin clay: Equilibrium and thermodynamic aspects. Chem. Int. 7, 139–144.

Awwad, A.M., Shammout, M.W., Amer, M.W., 2021. $Fe(OH)_3$/kaolinite nanoplatelets: Equilibrium and thermodynamic studies for the adsorption of Pb (II) ions from aqueous solution. Chem. Int. 7, 90–102.

Bayramoglu, G., Denizli, A., Bektas, S., et al, 2002. Entrapment of Lentinus sajor-caju into Ca-alginate gel beads for removal of Cd(II) ions from aqueous solution: preparation and biosorption kinetics analysis. Microchem. J. 72, 63–76.

Bhatti, H.N., Jabeen, A., Iqbal, M., et al, 2017. Adsorptive behavior of rice bran-based composites for malachite green dye: Isotherm, kinetic and thermodynamic studies. J. Mol. Liq. 237, 322–333.

Boumya, W., Khnifira, M., Machrouhi, A., et al, 2021. Adsorption of Eriochrome Black T on the chitin surface: experimental study, DFT calculations and molecular dynamics simulation. J. Mol. Liq. 331, 115706.

Daij, K.B., Bellebia, S., Bengharez, Z., 2017. Comparative experimental study on the COD removal in aqueous solution of pesticides by the electrocoagulation process using monopolar iron electrodes. Chem. Int. 3, 420–427.

Dubinin, M., Raduskhevich, L., 1947. Proceedings of the academy of sciences of the USSR. Phys Chem. 55, 327–329.

Elsherif, K.M., El-Dali, A., Alkarewi, A.A., et al, 2021. Adsorption of crystal violet dye onto olive leaves powder: Equilibrium and kinetic studies. Chem. Int. 7, 79–89.

Evy Alice Abigail, M. and R. Chidambaram, 2016. Rice husk as a low cost nanosorbent for 2,4-dichlorophenoxyacetic acid removal from aqueous solutions. Ecological Engineering. 92, 97-105.

Freundlich, H., 1906. Over the adsorption in solution. J. Phys. Chem. 57, 1100–1107.

Gupta, R.K., Singh, R.A., Dubey, S.S., 2004. Removal of mercury ions from aqueous solutions by composite of polyaniline with polystyrene. Sep. Purif. Technol. 38, 225–232.

Harkins, W.D., Jura, G., 1944. Surfaces of solids. XIII. A vapor adsorption method for the determination of the area of a solid without the assumption of a molecular area, and the areas occupied by nitrogen and other molecules on the surface of a solid. J. Am. Chem. Soc. 66, 1366–1373.

Ho, Y., McKay, G., 1999. Comparative sorption kinetic studies of dye and aromatic compounds onto fly ash. J. Environ. Sci. Health Part A. 34, 1179–1204.

Ho, Y., Ng, J., McKay, G., 2000. Kinetics of pollutant sorption by biosorbents. Sep. Purif. Methods 29, 189–232.

Ishtiaq, F., Bhatti, H.N., Khan, A., et al, 2020. Polypyrole, polyaniline and sodium alginate biocomposites and adsorption-desorption efficiency for imidacloprid insecticide. Int. J. Biol. Macromol. 147, 217–232.

Jalal, G., Abbas, N., Deeba, F., et al, 2021. Efficient removal of dyes in textile effluents using aluminum-based coagulants. Chem. Int. 7, 197–207.

Lammini, A., Dehbi, A., Omari, H., et al, 2022. DeExperimental and theoretical evaluation of synthetized cobalt oxide for phenol adsorption: Adsorption isotherms, kinetics, and thermodynamic studies. Arabian J. Chem., 104364.

Langmuir, I., 1918. The adsorption of gases on plane surfaces of glass, mica and platinum. J. Am. Chem. Soc. 40, 1361–1403.

Laonapakul, T., Suthi, T., Otsuka, Y., et al, 2022. Fluoride adsorption enhancement of Calcined-Kaolin/Hydroxyapatite composite. Arabian J. Chem. 15, 104220.

Maqbool, M., H. N. Bhatti, S. Sadaf, et al., 2020. Biocomposite of polyaniline and sodium alginate with Oscillatoria biomass: A potential adsorbent for the removal of basic blue 41. Journal of Materials Research and Technology. 9, 1 4 7 2 9 -1 4 7 4 1

Maqbool, M., Sadaf, S., Bhatti, H.N., et al, 2021. Sodium alginate and polypyrrole composites with algal dead biomass for the adsorption of Congo Red dye: kinetics, thermodynamics and desorption studies. Surf. Interfaces 25, 101183.

Minas, F., Chandravanshi, B.S., Leta, S., 2017. Chemical precipitation method for chromium removal and its recovery from tannery wastewater in Ethiopia. Chem. Int. 3, 392–405.

Naseer, A., Iqbal, M., Ali, S., et al, 2022. Green synthesis of silver nanoparticles using Allium cepa extract and their antimicrobial activity evaluation. Chem. Int. 8, 89–94.

Noreen, S., Zafar, S., Bibi, I., et al, 2022. ZnO, Al/ZnO and W/Ag/ZnO nanocomposite and their comparative photocatalytic and adsorptive removal for Turquoise Blue Dye. Ceram. Int. 48, 12170–12183.

Palanisamy, P., Agalya, A., Sivakumar, P., 2012. Polymer composite—a potential biomaterial for the removal of reactive dye. J. Chem. 9 (4), 1823–1834.

Salem, N.M., Awwad, A.M., 2022. Green synthesis and characterization of ZnO nanoparticles using Solanum rantonnetii leaves aqueous extract and antifungal activity evaluation. Chem. Int. 8, 12–17.

Salman, J.M., Al-Saad, K.A., 2012. Adsorption of 2, 4-dichlorophenoxyacetic acid onto date seeds activated carbon: equilibrium, kinetic and thermodynamic studies. Int. J. Chem. Sc. 10, 677–690.

Sasmaz, A., Sasmaz, B., Hein, J.R., 2021. Geochemical approach to the genesis of the Oligocene-stratiform manganese-oxide deposit, Chiatura (Georgia). Ore Geol. Rev. 128, 103910.

Sasmaz, M., Senel, G.U., Obek, E., 2020. Strontium accumulation by the terrestrial and aquatic plants affected by mining and municipal wastewaters (Elazig, Turkey). Environ. Geochem. Health 43, 1–14.

Sasmaz, M., Senel, G.U., Obek, E., 2021. Boron bioaccumulation by the dominant macrophytes grown in various discharge water environments. Bull. Environ. Contamin. Toxicol. 106, 1050–1058.

Sayed, M., 2015. Removal of ciprofloxacin by gamma irradiation: degradation mechanism and pathways of products studies. Chem. Int. 1, 81–86.

Şenol, Z.M., Keskin, Z.S., Özer, A., et al, 2022. Application of kaolinite-based composite as an adsorbent for removal of uranyl ions from aqueous solution: kinetics and equilibrium study. J. Radioanal. Nucl. Chem. 331, 403–414.

Şenol, Z.M., Şimşek, S., 2022. Insights into effective adsorption of lead ions from aqueous solutions by using chitosan-bentonite composite beads. J. Polym. Environ. 30, 3677–3687.

Shammout, M.W., Awwad, A.M., 2021. A novel route for the synthesis of copper oxide nanoparticles using Bougainvillea plant flowers extract and antifungal activity evaluation. Chem. Int. 7, 71–78.

Şimşek, S., Şenol, Z.M., Ulusoy, H.İ., 2017. Synthesis and characterization of a composite polymeric material including chelating agent for adsorption of uranyl ions. J. Hazard. Mater. 338, 437–446.

Şimşek, S., Kaya, S., Mine Şenol, Z., et al, 2022. Theoretical and experimental insights about the adsorption of uranyl ion on a new designed Vermiculite-Polymer composite. J. Mol. Liq. 352, 118727.

Temkin, M., 1940. Kinetics of ammonia synthesis on promoted iron catalysts. Acta Physiochim. URSS 12, 327–356.

Yadamari, T., Yakkala, K., Battala, G., Gurijala, R.N., 2011. Biosorption of malathion from aqueous solutions using herbal leaves powder. American J. Anal. Chem. 2 (08), 37.

Zeshan, M., Bhatti, I.A., Mohsin, M., et al, 2022. Remediation of pesticides using TiO2 based photocatalytic strategies: a review. Chemosphere 300, 134525.

Zhang, X., Han, R., 2022. Adsorption of 2, 4-dichlorophenoxyacetic acid by UiO-66-NH2 obtained in a green way. Environ. Sci. Pollut. Res., 1–14.